HHS Public Access

Author manuscript

J Biomater Sci Polym Ed. Author manuscript; available in PMC 2020 February 01.

Published in final edited form as:

J Biomater Sci Polym Ed. 2019 February ; 30(3): 215–232. doi:10.1080/09205063.2018.1563847.

Self-Assembled Monolayers of Phosphonates Promote Primary Chondrocyte Adhesion to Silicon Dioxide and Polyvinyl Alcohol Materials

Patrick E. Donnelly[a,b], **Laurianne Imbert**[c], **Kirsty L. Culley**[a], **Russell F. Warren**[a], **Tony Chen**[a,b], and **Suzanne A. Maher**[a,b,*]

[a]Orthopaedic Soft Tissue Research Program, Hospital for Special Surgery, New York, NY 10021, USA

[b]Department of Biomechanics, Hospital for Special Surgery, New York, NY 10021, USA

[c]Musculoskeletal Integrity Program, Hospital for Special Surgery, New York, NY 10021, USA

Abstract

The optimal solution for articular cartilage repair has not yet been identified, in part because of the challenges in achieving integration with the host. Coatings have the potential to transform the adhesive features of surfaces, but their application to cartilage repair has been limited. Self-assembled monolayer of phosphonates (SAMPs) have been demonstrated to increase the adhesion of various immortalized cell types to metal and polymer surfaces, but their effect on primary chondrocyte adhesion has not been studied. The objective of this study was to investigate the response of primary chondrocytes to SAMP coatings. We hypothesized a SAMP terminated with an α,ω-bisphosphonic acid, in particular butane-1,4-diphosphonic acid, would increase the number of adherent primary chondrocytes to polyvinyl alcohol (PVA). To test our hypothesis, we first established our ability to successfully modify silicon dioxide (SiO_2) surfaces to enable chondrocytes to attach to the surface, without substantial changes in gene expression. Secondly, we applied identical chemistry to PVA, and quantified chondrocyte adhesion. SAMP modification to SiO_2 increased chondrocyte adhesion by 3x after 4 hr and 4.5x after 24 hr. PVA modification with SAMPs increased chondrocyte adhesion by at least 31x after 4 and 24 hours. Changes in cell morphology indicated that SAMP modification led to improved chondrocyte adhesion and spreading, without changes in gene expression. In summary, we modified SiO_2 and PVA with SAMPs and observed an increase in the number of adherent primary bovine chondrocytes at 4 and 24 hr post-seeding. Mechanisms of chondrocyte interaction with SAMP-modified surfaces require further investigation.

Keywords

self-assembled monolayers; cartilage; chondrocytes; scaffolds; coatings; integration

*Author to whom correspondence should be addressed: Suzanne A. Maher, Hospital for Special Surgery, 535 East 70th Street, New York, NY 10021, 212 606 1083, MaherS@hss.edu.

DISCLOSURE STATEMENT

Suzanne A. Maher, Tony Chen, and Russel F. Warren are stock holders in AGelity Biomechanics.

1. INTRODUCTION

Isolated articular cartilage defects have been observed in up to 62% of patients under 40 years of age.[1–4] Due to its avascular nature and low cellular density, articular cartilage has a poor ability to repair, thus damage can spread from a focal lesion, eventually leading to osteoarthritis (OA).[1, 2, 4] Microfracture is a surgical technique used to treat such defects, in which the underlying bone is intentionally damaged to cause the formation of a blood clot to initiate a healing response. Despite its widespread use, microfracture can lead to variable levels of defect filling, with tissue that deteriorates after 2–5 years.[5] Replacement with autogenic and allogenic cartilage-bone (osteochondral) grafts have reported failure rates of 15–35% at 15 years.[6] While the reasons for failures are multifactorial, lack of integration between the graft and the host articular cartilage has been identified as a key factor.[7] Achieving integration with articular cartilage is particularly problematic for emerging technologies, like synthetic degradable and non-degradable scaffolds, which occasionally have surfaces that prevent chondrocyte and protein adhesion.[8–20]

Synthetic coatings have the potential to transform the cell adhesive features of a range of surfaces.[21–29] One coating in particular, self-assembled monolayer of phosphonates (SAMPs) can increase the adhesion of fibroblasts, osteoblasts, and stem cells, to both metal and polymer surfaces, without changing bulk mechanical properties or surface roughness.[30–36] The termination group added to SAMPs can be controlled depending on the desired adhesion, but α,ω-bisphosphonic acids have been used most commonly. SAMP-coated titanium alloy surfaces terminated with an α,ω-bisphosphonic acid and Arg-Gly-Asp (RDG) tripeptide have demonstrated increased *in vivo* bone deposition and superior interfacial strength compared to hydroxyapatite coatings.[37] Surface patterning of α,ω-bisphosphonic acid SAMPs on oxide and polymer surfaces have also been shown to direct fibroblasts and stem cell adhesion and proliferation to modified surfaces, which in turn promoted spatially defined assembly of ECM.[38, 39] While surfaces modified with RGD/fibronectin and chitosan have been shown to increase chondrocyte adhesion [40–42], primary chondrocyte affinity to α,ω-bisphosphonic acid SAMP modified surfaces has not been investigated.

Poly(vinyl alcohol), PVA, is a synthetic material that has garnered recent interest as a candidate material for cartilage replacement.[43] While studies have shown that PVA placed in contact with blood serum can cause complement activation in the pancreas [44, 45], recent FDA approval of a PVA synthetic cartilage device, Cartiva® for osteoarthritis of the big toe,[46] indicate that international standards for biocompatibility (ISO 10993) have been met for its use in the environment of diarthroidal joints. However, PVA has a non-protein adsorptive and non-cell adhesive surface, which in some instances can lead to *in vivo* fibrous encapsulation and implant loosening [47, 48]. As such, PVA-cartilage integration could potentially benefit from the incorporation of α,ω-bisphosphonic acid SAMPs.

The objective of this study was to investigate the response of primary chondrocytes to SAMP coatings. We hypothesized that a SAMP terminated with an α,ω-bisphosphonic acid, in particular butane-1,4-diphosphonic acid, would increase the number of adherent primary chondrocytes to PVA. To test our hypothesis, we first established our ability to successfully modify silicon dioxide (SiO_2) surfaces so that chondrocytes could attach to the surface and

remain viable, without substantial changes in gene expression. Secondly, we applied identical chemistry to PVA, and quantified chondrocyte adhesion and morphology as a function of post-cell seeding time, and cell viability.

2. MATERIALS AND METHODS

2.1 General

Hexanes, toluene, methanol, 2-propanol, concentrated sulfuric acid, 30% hydrogen peroxide (Acros Organics); p-type, boron-doped silicon terminated with 1000 Å thermal oxide (University Wafer, Inc.); absolute ethanol, 10% formalin solution (Pharmco-Aaper); zirconium(IV) *tert*-butoxide, poly(vinyl alcohol) (M_W 89,000–98,000; PVA), 88% formic acid, butane-1,4-diphosphonic acid, octadecylphosphonic acid, typan blue, bovine serum albumin (BSA), TWEEN® 20, Triton™ X-100 (Sigma-Aldrich); collagenase type II (Worthington Biochemical Corp.) commercial grade and zero-grade nitrogen gas (TW Smith); Dulbecco's Modified Eagle Medium (DMEM)/F12, DMEM, (Gibco Laboratories); fetal bovine serum (FBS, Atlanta Biologicals); ProLong® Gold Antifade Mountant with DAPI, trypsin, penicillin-streptomycin, LIVE/DEAD® Cell Imaging Kit (ThermoFisher Scientific); actin cytoskeleton/focal adhesion staining kit (MilliporeSigma); TRIzol® reagent (Life Technologies); RNeasy Plus minikit (Qiagen). All chemicals were used without further purification, unless otherwise noted. Mature bovine knees were obtained from a local abattoir.

2.2 Silicon Substrate Cleaning

Silicon substrates were cleaned following previously published methods.[38] In brief, silicon wafers were diced into 1 cm x 1 cm chips and cleaned by sequential sonication in hexanes, toluene, and methanol for 15 min each. The silicon substrates were then rinsed with 2-propanol and dried under a stream of nitrogen before immersion in "piranha acid" solution (H_2SO_4: 30% H_2O_2, 3:1) at 85 °C for 15 min. The substrates were then rinsed sequentially with deionized water and 2-propanol, and dried under a stream of nitrogen. The clean silicon substrates were stored in a vacuum desiccator until use.

2.3 Chemical Vapor Deposition of Zirconium(IV) *Tert*-Butoxide (1), and Synthesis of Self-Assembled Monolayers of Phosphonates (4,5)

See Figure 1 for a schematic and numbering conventions. Substrate surfaces were modified following previously published methods.[38, 49] In brief, clean substrates (silicon or PVA film) were placed inside a custom-built chemical vapor deposition chamber equipped with two valves; one connected to vacuum and the other connected to a bulb containing zirconium(IV) *tert*-butoxide (**1**). The deposition chamber was pumped down to 1 mtorr for 15 min, the valve was open to the bulb containing **1** for 3–5 min with the valve to the vacuum remaining open, both valves were then closed and the chamber was heated. Substrates to be modified with SAMPs were heated to 50 °C to assemble a mixed alkoxide/oxide layer (**2**) while substrates to be terminated with a zirconium oxide layer (**3**) prior to polymer film casting were heated to 80 °C to ensure complete thermolysis of the alkoxide. The chamber was allowed to cool to room temperature, and then cleared by opening the vacuum valve. The chamber was then backfilled with zero-grade nitrogen. Substrates to be

modified with butane-1,4-diphosphonic acid (**4**) were quickly removed from the chamber and immersed in a solution of the phosphonic acid in absolute ethanol (0.25 mg/mL), substrates terminated with **3** were placed in deionized water; all substrates were immersed in solution overnight, except for modified-PVA films which were removed after 2 hr. Substrates were then sonicated in ethanol for 15 min, rinsed sequentially with ethanol and 2-propanol, and dried under a stream of nitrogen; all substrates were stored in a vacuum desiccator until use.

2.4 PVA Film Casting

PVA thin films were prepared based on previously published methods.[49] In brief, **3**-terminated silicon substrates were rinsed sequentially with deionized water, ethanol, and 2-propanol and dried under a stream of nitrogen. A 20% (w/v) PVA solution was prepared with 88% formic acid. PVA films were spin cast by applying 10 drops of the PVA solution to the **3**-terminated silicon substrates while spinning at 3200 rpm for 60 sec. The PVA-coated substrate was heated at 120 °C for 10 min and then cooled to room temperature. PVA substrates were stored in a vacuum desiccator until use.

2.5 Surface Characterization

The water wetting contact angle of unmodified and modified PVA substrates was measured using a house-built contact angle goniometer.[50] For the purposes of surface characterization, an additional formulation was created, where the butane-1,4-diphophonic acid (a hydrophilic SAMP) was instead replaced with octadecylphosphonic acid (**5**, a hydrophobic SAMP) – a highly hydrophobic moiety. This addition was used as a positive control, so that visual confirmation of the presence of SAMP could be made. A drop of deionized water (5 μL) was applied to each substrate surface and an image was captured using a Casio Exilim EX-ZS5 14.1 megapixel digital camera. The contact angle was measured using ImageJ software and the “Contact Angle” analysis script.[51, 52] X-Ray photoelectron spectroscopy (XPS) analysis was performed on substrates using a ThermoFisher K-Alpha X-Ray Photoelectron Spectrometer with an Al Kα source. Survey scans were collected by averaging 5 scans at 200 eV pass energy, 10 ms dwell time, 1 eV step size, and a 400 μm spot size from 1350 eV to −10 eV. Detailed, elemental scans were collected by averaging 10 scans at 50 eV pass energy, 50 ms dwell time, 0.1 eV step size, and a 400 μm spot size. Data analysis was conducted using CasaXPS software (Casa Software, Ltd.). XP spectra were calibrated against the adventitious C 1s (284.5 eV). Scanning electron microscopy (SEM) analysis was performed on a FEI Quanta 200 Environmental SEM at an acceleration voltage of 10.00 keV in low vacuum mode with water vapor at 0.53 torr. Atomic force microscopy (AFM) was performed using an Anasys Instruments nanoIR2™ operating in tapping mode; scan rate = 0.3–0.5 KHz, resolution was 500 pt (X) and 300 pt (Y). Data analysis was performed using Analysis Studio Software (Anasys Instruments). Surface roughness and PVA film thickness are reported as the average ± 1 standard deviation of 5 individual measurements.

2.6 Primary Chondrocyte Isolation

Primary chondrocytes were isolated from mature bovine cartilage taken from the femoral condyles as previously described.[53] In brief, isolated cartilage was digested in 500 U/mL Collagenase Type II overnight at 37 °C in an atmosphere of 5% CO_2. The digested cartilage was then passed through a 70 μM cell strainer and viability assessed by typan blue staining. Passage 0 primary chondrocytes were then seeded at 200,000 cells/cm^2 in complete media consisting of Dulbecco's modified Eagle's medium (DMEM)-Ham's F-12 (1:1, v/v) and 10% (v/v) fetal bovine serum (FBS), supplemented with penicillin-streptomycin. Chondrocytes were used at passage 1 for all experiments.

2.7 Chondrocyte Adhesion Study and Staining

4-Terminated and unmodified SiO_2 and PVA substrates (Figure 1) were placed into 24-well tissue culture plates and rinsed with 70% (v/v) ethanol in water and allowed to air dry, the substrates were then rinsed with sterile 1x PBS. Chondrocytes were seeded onto the substrates at 30,000 cells/mL/well. Cells were allowed to adhere for 4 hr, after which time the media was changed to remove unattached cells and replaced with fresh complete media. After 4 and 24 hr substrates were removed from each group and stained to visualize chondrocytes. Cell adhesion experiments were performed in duplicate on both SiO_2 and PVA, at least 3 substrates per experiment ($n \geq 6$ substrates total).

Chondrocytes were stained as follows: surfaces were rinsed twice with PBS/TWEEN 20 (0.05%, v/v), and then adhered cells were fixed with 10% (v/v) formalin for 15 min at room temperature. Substrates were rinsed twice again with PBS/TWEEN 20, followed by cell permeabilization with 0.1% (v/v) Triton X-100 in PBS for 5 min at room temperature. Surfaces were then rinsed twice with PBS/TWEEN 20 and then blocked with PBS/BSA (1%, w/v) for 30 min. Cells were stained with rhodamine phallodin (1:50, PBS/BSA 2%, w/v) at room temperature for 60 min, then rinsed sequentially three times in PBS and finally in deionized water. For imaging, substrates were adhered face-up to glass slides and mounted using ProLong Gold antifade medium with DAPI. Chondrocytes cultured on PVA were also stained for viability using a LIVE/DEAD® Cell Imaging Kit following the directions provided by the manufacturer. Images were captured using a Nikon Eclipse Ni-E microscope. Relative cell adhesion was determined by counting the number of cell nuclei in each image. Three substrates were analyzed for each group at each time point, and 2–3 images were captured at 20x magnification; therefore, $n \geq 12$ images for cell adhesion experiments and $n \geq 8$ for cell viability experiments.

2.8 Gene expression assays

Passage 1 chondrocytes were plated in complete media at 30,000 cells/mL/well onto SAMP-modified and unmodified SiO_2 surfaces, contained within 24-well plates or directly onto tissue culture plastic (control). Cells adhered to the surfaces were harvested into TRIzol® reagent at 3 days post seeding, and samples stored at −80°C until RNA isolation.

2.9 Real-time Quantitative RT-PCR (RT-qPCR) Analysis

Total RNA was isolated from chondrocytes using TRIzol® reagent followed by DNaseI treatment and column clean-up via the RNeasy Plus minikit. RNA (150ng) was then reverse transcribed using iScript RT Supermix for RT-qPCR (Bio-Rad) following manufacturer's instructions. Amplifications were carried out using SsoAdvanced Universal SYBR Green (Bio-Rad)-based real-time PCR on the CFX96™ Real-Time PCR detector system (Bio-Rad). PCR primers (described in Table 1) were used at an annealing temperature of 60°C. The data were calculated as the ratio of each gene to Rpl13a using the 2-ΔΔCt method for relative quantification, with Gapdh used as additional housekeeping control genes.

2.10 Data and Statistical Analyses

The adhesion cell count data was averaged and all data was normalized to the 4 hr control group. Gene expression data was normalized to gene expression of Rpl13a for each sample. Data are reported as average ± 1 standard error of the mean (S.E.). Statistical analysis was performed using one-way analysis of variance (ANOVA) with Tukey Post-Hoc testing, $\alpha = 0.05$. Statistical analyses were performed with GraphPad Prism 6.0. P values less than or equal to 0.05 were considered significant.

3. RESULTS

3.1 Surface Characterization SiO_2 & PVA Surfaces

4-Terminated PVA films were analyzed sequentially starting from clean SiO_2, building the surface chemistry up to **4**-terminated PVA (Figure 2). The XP spectrum of clean, unmodified SiO_2 is shown in Figure 2A, Si(2s) and Si(2p) peaks were observed at 155 eV and 104 eV, respectively. The peak at approximately 24 eV was assigned to the O(2s). Of note, the O(2s) peak shifted slightly as the surface continued to be coated with the Zr oxide/alkoxide and PVA. The shift is likely due to the surface becoming more insulating and the presence of additional oxygen containing species from the Zr oxide/alkoxide layer and the PVA thin film. Figure 2B shows the spectrum of **3**-modified SiO_2, here the Si peaks are still visible and the Zr(3d) is observed at 183 eV; the $Zr(3d_{5/2})$ and $Zr(3d_{3/2})$ were not resolved. The peak at 197 eV was assigned to a Zr plasmon loss. The spectrum of a **3**-modified SiO_2 surface coated with a PVA film is shown in Figure 2C, Si and Zr peaks were no longer visible. In Figure 2D the Zr(3d) is visible again for **3**-modified PVA film. The spectrum of **4**-terminated PVA shows the Zr(3d) peak along with the P(2p) at 134 eV, the P(2s) was also visible at 190 eV supporting successful SAMP surface modification, Figure 2E. The water wetting contact angle was measured for PVA film substrates, and **4**-terminated and **5**-terminated PVA (Figure 3A–C). The contact angle of the unmodified PVA film was 56°, **4**-terminated PVA < 20°, and **5**-terminated PVA > 100°. Atomic force microscopy measured the surface roughness of the PVA films to be 3.5 nm ± 0.7 nm. PVA film thickness was measured at 123 nm ± 2 nm (Figure 3D–E).

3.2 Chondrocyte Adhesion to 4-Terminated and Unmodified SiO_2 Surfaces

After 4 hr, 2.7 ± 0.1 times more chondrocytes were adhered to **4**-terminated SiO_2 when compared to unmodified surfaces. At 24 hr 4.7 ± 0.2 times more chondrocytes cells were

adhered to **4**-terminated surfaces than unmodified surfaces (Figure 4A–E). The cell count on the **4**-terminated SiO_2 was significantly different from the controls at both time points, $p < 0.001$. Cell morphology was notably different on each surface and changed with time. After 4 hr, chondrocytes adhered to unmodified SiO_2 had a predominantly rounded morphology, and were not well-spread, whereas cells adhered to **4**-terminated SiO_2 were found to be spread and spindle shaped, with only a few round cells observed. After 24 hr, adhered chondrocytes were spindle shaped on the unmodified SiO_2 with some still remaining round. On the **4**-terminated SiO_2 the cells remained spread and spindle shaped with a few round cells remaining (Figure 4B–E). Magnified 20x images are shown in Figure 5 to demonstrate focal adhesions stained with anti-vinculin antibodies. Focal adhesions were only noted in cells that were attached and had begun to spread.

3.3 Chondrocyte Adhesion to 4-Terminated and Unmodified PVA film Surfaces

After 4 hr, 31 ± 4 times more chondrocytes were adhered to **4**-terminated PVA films than unmodified PVA, which had very few cells attached. Some images collected of unmodified PVA had no cells within the region of interest (Figure 6A–E). Within 24 hr, the number of cells adhered to the unmodified PVA was statistically unchanged from the 4 hr time point, but 45 ± 6 times more cells adhered to the **4**-terminated surface than the unmodified surface. Cell morphology was similar on both unmodified and **4**-terminated PVA surfaces with round cells observed after 4 and 24 hr. A few cells were observed beginning to spread on the **4**-terminated PVA surfaces at 24 hr but were not spindle shaped (Figure 6B–E).

3.4 Chondrocyte Viability on 4-Terminated and Unmodified PVA Surfaces

Chondrocytes were stained after 4 and 24 hr in culture on unmodified and **4**-terminated PVA. After 4 hr, 100% of the cells on unmodified PVA were found to be viable and 98% ± 2% were viable on the **4**-terminated surfaces (n = 4 surfaces, 8 = images). After 24 hr, 100% of the cells on unmodified PVA were viable and 97% ± 6% were viable on **4**-terminated PVA.

3.5 Chondrocyte Gene Expression to 4-Terminated and Unmodified SiO_2 Surfaces

After 3 days, a 2.9 ± 0.9 times decrease in Col1a2 gene expression was observed in chondrocytes plated on the unmodified SiO_2 surfaces compared to both the control (tissue culture plastic) and **4**-terminated surfaces ($p<0.05$) (Figure 7B). There were no significant differences in gene expression between groups for Col2a1, Acan, Sox9, or Runx2 (Figure 7A, C-E). There were differences found between tissue culture plastic and **4**-terminated surfaces.

4. DISCUSSION

The objective of this study was to investigate the response of primary chondrocytes to SAMP coatings. We hypothesized that a SAMP terminated with an α,ω-bisphosphonic acid, in particular butane-1,4-diphosphonic acid, would increase the number of adherent primary chondrocytes to PVA. To test our hypothesis, we first established our ability to successfully modify silicon dioxide (SiO_2) surfaces and demonstrated that chondrocytes attached to the surface with a two-to-four fold increase relative to untreated surfaces. The cells remained

viable, expressed vinculin, and although changed morphologically, did not change their gene expression profiles. When identical chemistry was applied to PVA, a 45-fold increase in the number of adherent cells at 24 hours post-seeding relative to the untreated surfaces occurred.

SAMP surface modifications result in nanometer thin molecular layers that can change the surface properties of materials to significantly influence cell interactions, without changing bulk mechanical properties.[38] SAMPs have been shown to be as effective at increasing cell adhesion as the RGD tripeptide, with the added benefit that bisphosphonic acids are abiologic and as such, more stable and easily stored.[35] By increasing the affinity of cells to material surfaces, the integration of implanted devices may be enhanced, which has been demonstrated for integration of surfaces with bone via osteoblast adhesion, *in vitro* and *in vivo*.[31, 37] SAMP modification can be performed on nearly any material surface that possesses repeating electron-rich functionality. Surface modification with SAMPs has been reported to increase cell affinity to polymer surfaces of PET, PEEK, and nylon 6,6, as well as other metal oxide surfaces, and osteoblasts, fibroblasts, and stems cells have been shown to respond positively (increased adhesion) to surfaces modified with SAMPs of bisphosphonic aicds, such as termination **4** used in this study.[30–36] Spatial modification of surfaces with **4** have been shown to control cell adhesion and spatially direct cell proliferation, such that the adherent cells developed spatially aligned ECM and direct neurite outgrowth.[38, 39, 54, 55] It should be noted that the α,ω-bisphosphonic acid used in the work, butane-1,4-diphosphonic acid, is not a therapeutic bisphosphonic acid, as those commonly used to treat inflammatory joint diseases or osteoporosis. Further, the SAMPs are surface bound and not free floating in media. Previous work has found that the surface loading of butane-1,4-diphosphonic acid was 0.40 ± 0.03 nmol/cm^2, as measured using a quartz crystal microbalance.[36]

While other cells types have been studied, the response of primary chondrocytes to SAMP modified surfaces has not been analyzed. Given the ongoing efforts to engineer the interface between scaffolds/ implants and host articular cartilage into which they are implanted,[56–58] the potential application of SAMPs to encourage chondrocyte adhesion is of translational relevance in the field of orthopaedic surgery.

SAMP coatings were applied to both SiO_2 and PVA materials. The main purpose of the SiO_2 material was to demonstrate the feasibility of creating the surface modification in our laboratory, and to provide evidence that the surface was not cytotoxic to primary chondrocytes. We also use the opportunity to study the adhesion of chondrocytes and their gene expression profiles. SiO_2, to which chondrocytes already have some ability to adhere, has been characterized and studied with SAMP modification for cell adhesion previously.[38] In this study, we found that modification increased primary chondrocyte adhesion by about 3x after 4 hr and 4.5x after 24 hours compared to the native SiO_2. We also observed that as the chondrocytes began to spread on the surfaces, that focal adhesions became visible using an anti-vinculin stain. Previous work with NIH 3T3 fibroblasts and immortalized osteoblasts also found the formation of focal adhesions to other SAMP surface modifications.[32, 34–36] Chondrocytes appeared to have a fibroblast-like morphology when adhered to the modified SiO_2 surface and it was unclear if this was due to the SAMP, surface stiffness, or due to low chondrocyte density, as chondrocytes have been shown to

dedifferentiate at low density.[59] However, it was important to use low seeding density in order to find differences in adhesion to the surface alone and not as a result of cell-cell interactions, which would occur when cells are seeded in high density.

Armed with this information, identical surface chemistry was applied to PVA. PVA was chosen because it has been studied and approved as a permanent replacement for articular cartilage due to its mechanical characteristics,[43, 60, 61] and yet it is recognized that chondrocytes cannot attach to its surface. We demonstrated that our method of manufacture, based on a method developed by Jones et al.,[49] resulted in a smooth, stable surface with an average surface roughness of 3.5 nm. Water wetting contact angle goniometry supported successful SAMP modification of PVA films, and XPS analysis of **4**-terminated PVA films showed the presence of Zr and P on the surface, further supporting successful modification of the PVA surface. As expected, very few chondrocytes adhered to the native PVA surfaces, and those that did adhere remained chondrocyte-like, indicated by rounded cell morphology. The **4**-terminated PVA surfaces were more than 30x more adhesive than the unmodified PVA after 4 hr and 24h, and the cells maintained their rounded morphology.

There was an observed difference in chondrocyte morphology between chondrocytes cultured on **4**-terminated SiO_2 and PVA surfaces. These differences can be attributed to several factors: the studies were conducted on flat surfaces at low-seeding densities, and not three-dimensional gels, scaffolds, or in micromass that chondrocytes are typically cultured in[62–64] and as such, changes in morphology away from the more typical rounded shape are not surprising. The spindle-like morphology and the spreading of cells on the modified SiO_2 surfaces suggested a fibroblast-like phenotypic shift of the cells respectively. To assess whether such a changes occurred, real-time quantitative RT-PCR (RT-qPCR) analysis was completed to assess the gene expression of chondrocytes cultured on standard tissue culture plastic (TCP), **4**-terminated SiO_2 and unmodified SiO_2 surfaces after 3 days of culture. The genes analyzed (type I collagen (Col1a2), type II collagen (Col2a1), Aggrecan (Acan), Runx2, and Sox9) represent those that delineate the transition of normal chondrocytes to hypertrophic chondrocytes or dedifferentiation to fibroblast-like cells due to either their decrease or increased expression. We found no significant differences in chondrogenic or hypertrophic gene expression between chondrocytes cultured on TCP and **4**-terminated SiO_2 but a difference of the dedifferentiation marker Col1a2 between chondrocytes cultured on unmodified SiO_2 and the other 2 conditions. These results suggest that bisphosphonic acid SAMP modification does not induce phenotypic change of chondrocytes any more than tissue culture plastic, and that the morphological differences are likely due to dedifferentiation of the chondrocytes into a more fibroblast-like cell when cultured on a cell-adherent stiff substrate.[65, 66] This finding is further noted by the morphological differences noted between modified SiO_2 and modified PVA – where chondrocytes cultured on SiO_2 have a more fibroblastic morphology, that is not seen for chondrocytes cultured on modified PVA which has a much lower stiffness – PVA films have a Young's modulus ranging from 1.50–3.75 GPa, while that of silicon ranges from 130–188 GPa.[67, 68]

The mechanism by which SAMPs activate surfaces towards cell adhesion is unknown. However, it is likely multifactorial depending on differential protein adsorption and, potentially, changes in protein confirmation when adsorbed to surfaces, exposing cell

adhesive moieties. Previous studies using SAMPs for cell adhesion or matrix deposition have relied on the use of immortalized cell lines; for example, NIH 3T3 fibroblasts.[34–36, 38, 39, 55] In this work we sought to use primary mature bovine chondrocytes, which have different properties compared to immortalized lines. It has been shown that immortalized lines differ from primary cell in both surface adherence and their general metabolism.[69] Further, there is variability among primary cells taken from different donor animals, which makes their behavior difficult to predict.[69] However, we have found that while there is variability in the native adherence of the primary chondrocytes to the surfaces in general, that SAMP coatings will increase the number of adherent cells. To our knowledge, this is the first example using primary chondrocytes to investigate the ability of α,ω-bisphosphonic acid SAMPs to increase primary chondrocyte adhesion.

Our research had the following limitations. All cell experiments were performed *in vitro*, and the results from these may not translate to the *in vivo* setting since the *in vivo* environment is significantly more complex from a biological and mechanical standpoint. Furthermore, the two dimensional nature of the materials that were modified does not allow for an assessment of the integrative capacity of cells once they are adhered to the surface. Additionally, the cell morphology was only observed using immunofluorescence at a relatively low magnification (20x), additional experiments observing morphology via scanning electron microscopy are needed. The gene expression study was only performed on SiO_2 and not on PVA. While the data obtained on SiO_2 is interesting and useful, having performed the same study on cells attached to PVA would be beneficial. This experiment was not performed in the present study because the solvent used to isolate the chondrocyte DNA (TRIzol®) caused the PVA thin films to delaminate and dissolve, causing the cells to be lost. Further, the unmodified PVA had so few chondrocytes attached that there was not a suitable control for comparison.

5. CONCLUSIONS

In this work we sought to determine if a SAMP surface coating of an α,ω-bisphosphonic acid would increase primary chondrocyte adhesion to PVA. Primary chondrocyte response to cell-adhesive SAMP coatings was modeled on an oxide surface (SiO_2), and on a polymer surface (PVA). We found that SAMP coatings significantly increased chondrocyte adhesion relative to untreated SiO_2, which itself is moderately cell-adhesive. Stable, thin film surfaces of PVA were fabricated, characterized, and successfully modified with SAMPs. Primary chondrocyte adhesion was significantly increased on SAMP-modified PVA surfaces. The results of this study suggest that SAMP modification of PVA surfaces with α,ω-bisphosphonic acids, can be used to increase the adhesion of chondrocytes to surfaces of material that are otherwise not cell adhesive. Increasing cell affinity to the surfaces of implanted materials is a critical component of successful biointegration, since cells on the surfaces of implants can secrete and assemble ECM that can fill any interfacial gap.[7, 70] Many polymers, like PVA, have mechanical properties that render them suitable for cartilage replacement, but have surface properties that discourage cell adhesion. SAMP surface modification may be a useful approach to enable these polymeric materials to biologically integrate with the host tissue.

ACKNOWLEDGEMENTS

The authors thank Dr. Adele Boskey (Hospital for Special Surgery, New York, NY) for equipment/instrument use, and Prof. Jeffrey Schwartz and Ms. Kelly Lim (Princeton University, Princeton, NJ) for assistance and use of equipment.

FUNDING

Support for this study was made possible by Grant Number T32 AR007281, Musculoskeletal Training from the National Institutes of Health – National Institute of Arthritis and Musculoskeletal Skin Diseases. We thank the Russell Warren Chair in Tissue Engineering for supporting this research.

REFERENCES

[1]. Flanigan DC, Harris JD, Trinh TQ, Siston RA, Brophy RH. Prevalence of chondral defects in athletes' knees: a systematic review. Med. Sci. Sports Exerc 2010;42(10):1795–801. [PubMed: 20216470]

[2]. Bhosale AM, Richardson JB. Articular cartilage: structure, injuries and review of management. Br. Med. Bull 2008;87(1):77–95. [PubMed: 18676397]

[3]. Montgomery SR, Foster BD, Ngo SS, Terrell RD, Wang JC, Petrigliano FA, et al. Trends in the surgical treatment of articular cartilage defects of the knee in the United States. Knee Surg. Sports Traumatol. Arthrosc 2014;22(9):2070–5. [PubMed: 23896943]

[4]. Emans PJ, van Rhijn LW, Welting TJ, Cremers A, Wijnands N, Spaapen F, et al. Autologous engineering of cartilage. Proc. Natl. Acad. Sci. U. S. A 2010;107(8):3418–23. [PubMed: 20133690]

[5]. Gobbi A, Karnatzikos G, Kumar A. Long-term results after microfracture treatment for full-thickness knee chondral lesions in athletes. Knee Surg. Sports Traumatol. Arthrosc 2014;22(9): 1986–96. [PubMed: 24051505]

[6]. Cole BJ, Pascual-Garrido C, Grumet RC. Surgical management of articular cartilage defects in the knee. JBJS. 2009;91(7):1778–90.

[7]. Khan I, Gilbert S, Singhrao S, Duance V, Archer C. Cartilage integration: evaluation of the reasons for failure of integration during cartilage repair. A review. European cells & materials 2008;16(2).

[8]. Dawson CK, Rolf RH, Holovacs TF. The Management of Localized Articular Cartilage Lesions of the Humeral Head in the Athlete. Oper. Tech. Sports Med 2008;16(1):14–20.

[9]. Miniaci A Arthrosurface Inlay Resurfacing: Indications, Surgical Technique, and Results. Small Implants in Knee Reconstruction: Springer; 2013 p. 125–36.

[10]. Baker MI, Walsh SP, Schwartz Z, Boyan BD. A review of polyvinyl alcohol and its uses in cartilage and orthopedic applications. Journal of Biomedical Materials Research Part B: Applied Biomaterials. 2012;100B(5):1451–7.

[11]. Cheng G, Davoudi Z, Xing X, Yu X, Cheng X, Li Z, et al. Advanced Silk Fibroin Biomaterials for Cartilage Regeneration. ACS Biomaterials Science & Engineering. 2018;4(8):2704–15.

[12]. Cheng G, Chen J, Wang Q, Yang X, Cheng Y, Li Z, et al. Promoting osteogenic differentiation in pre-osteoblasts and reducing tibial fracture healing time using functional nanofibers. Nano Research. 2017:1–20.

[13]. Wang Q Smart Materials for Tissue Engineering: Applications: Royal Society of Chemistry; 2017.

[14]. Shi Z, Gao X, Ullah MW, Li S, Wang Q, Yang G. Electroconductive natural polymer-based hydrogels. Biomaterials. 2016;111:40–54. [PubMed: 27721086]

[15]. Hu X, Tang Y, Wang Q, Li Y, Yang J, Du Y, et al. Rheological behaviour of chitin in NaOH/urea aqueous solution. Carbohydr. Polym 2011;83(3):1128–33.

[16]. Lamboni L, Gauthier M, Yang G, Wang Q. Silk sericin: a versatile material for tissue engineering and drug delivery. Biotechnol. Adv 2015;33(8):1855–67. [PubMed: 26523781]

[17]. Wang Q, Du Y-m, Fan L-h, Liu H, Wang X-h. Structures and Properties of Chitosan-Starch-Sodium Benzoate Blend Films [J]. Wuhan University Journal (Natural Science Edition). 2003;6:013.

[18]. Peng H, Poovaiah N, Forrester M, Cochran E, Wang Q. Ex vivo culture of primary intestinal stem cells in collagen gels and foams. ACS Biomaterials Science & Engineering. 2014;1(1):37–42.

[19]. Wang Q, Jamal S, Detamore MS, Berkland C. PLGA-chitosan/PLGA-alginate nanoparticle blends as biodegradable colloidal gels for seeding human umbilical cord mesenchymal stem cells. Journal of biomedical materials research Part A. 2011;96(3):520–7. [PubMed: 21254383]

[20]. Wang Q Smart Materials for Tissue Engineering: Fundamental Principles: Royal Society of Chemistry; 2016.

[21]. Mrksich M A surface chemistry approach to studying cell adhesion. Chem. Soc. Rev 2000;29(4): 267–73.

[22]. Ku SH, Ryu J, Hong SK, Lee H, Park CB. General functionalization route for cell adhesion on non-wetting surfaces. Biomaterials. 2010;31(9):2535–41. [PubMed: 20061015]

[23]. Faucheux N, Schweiss R, Lützow K, Werner C, Groth T. Self-assembled monolayers with different terminating groups as model substrates for cell adhesion studies. Biomaterials. 2004;25(14):2721–30. [PubMed: 14962551]

[24]. Guo S, Zhu X, Loh XJ. Controlling cell adhesion using layer-by-layer approaches for biomedical applications. Materials Science and Engineering: C. 2017;70:1163–75. [PubMed: 27772718]

[25]. Ma Z, Mao Z, Gao C. Surface modification and property analysis of biomedical polymers used for tissue engineering. Colloids Surf. B. Biointerfaces 2007;60(2):137–57. [PubMed: 17683921]

[26]. Yuan L, Yu Q, Li D, Chen H. Surface Modification to Control Protein/Surface Interactions. Macromol. Biosci 2011;11(8):1031–40. [PubMed: 21337519]

[27]. Lee W-H, Loo C-Y, Rohanizadeh R. A review of chemical surface modification of bioceramics: Effects on protein adsorption and cellular response. Colloids Surf. B. Biointerfaces 2014;122:823–34. [PubMed: 25092582]

[28]. Dennes TJ, Schwartz J. A nanoscale metal alkoxide/oxide adhesion layer enables spatially controlled metallization of polymer surfaces. ACS applied materials & interfaces. 2009;1(10): 2119–22. [PubMed: 20355844]

[29]. Khan S, Newaz G. A comprehensive review of surface modification for neural cell adhesion and patterning. Journal of Biomedical Materials Research Part A. 2010;93A(3):1209–24.

[30]. Schwartz J, Avaltroni MJ, Danahy MP, Silverman BM, Hanson EL, Schwarzbauer JE, et al. Cell attachment and spreading on metal implant materials. Materials Science and Engineering: C. 2003;23(3):395–400.

[31]. Gawalt E, Avaltroni M, Danahy M, Silverman B, Hanson E, Midwood K, et al. Bonding organics to Ti alloys: facilitating human osteoblast attachment and spreading on surgical implant materials corrections. Langmuir. 2003;19(17):7147-.

[32]. Dennes TJ, Hunt GC, Schwarzbauer JE, Schwartz J. High-yield activation of scaffold polymer surfaces to attach cell adhesion molecules. J. Am. Chem. Soc 2007;129(1):93–7. [PubMed: 17199287]

[33]. Allon AA, Ng KW, Hammoud S, Russell BH, Jones CM, Rivera JJ, et al. Augmenting the articular cartilage-implant interface: Functionalizing with a collagen adhesion protein. Journal of Biomedical Materials Research Part A. 2012;100(8):2168–75. [PubMed: 22615182]

[34]. Dennes TJ, Schwartz J. Controlling cell adhesion on polyurethanes. Soft Matter. 2008;4(1):86–9.

[35]. Dennes TJ, Schwartz J. A nanoscale adhesion layer to promote cell attachment on PEEK. J. Am. Chem. Soc 2009;131(10):3456–7. [PubMed: 19275255]

[36]. Danahy MP, Avaltroni MJ, Midwood KS, Schwarzbauer JE, Schwartz J. Self-assembled monolayers of alpha,omega-diphosphonic acids on Ti enable complete or spatially controlled surface derivatization. Langmuir. 2004;20(13):5333–7. [PubMed: 15986670]

[37]. Shannon FJ, Cottrell JM, Deng XH, Crowder KN, Doty SB, Avaltroni MJ, et al. A novel surface treatment for porous metallic implants that improves the rate of bony ongrowth. Journal of Biomedical Materials Research Part A. 2008;86(4):857–64. [PubMed: 18041733]

[38]. Donnelly PE, Jones CM, Bandini SB, Singh S, Schwartz J, Schwarzbauer JE. A Simple Nanoscale Interface Directs Alignment of a Confluent Cell Layer on Oxide and Polymer

Surfaces. Journal of materials chemistry. B, Materials for biology and medicine. 2013;1(29): 3553–61. [PubMed: 23936630]

[39]. Singh S, Bandini SB, Donnelly PE, Schwartz J, Schwarzbauer JE. A cell-assembled, spatially aligned extracellular matrix to promote directed tissue development. Journal of materials chemistry. B, Materials for biology and medicine. 2014;2(11):1449–53. [PubMed: 24707354]

[40]. Genes NG, Rowley JA, Mooney DJ, Bonassar LJ. Effect of substrate mechanics on chondrocyte adhesion to modified alginate surfaces. Arch. Biochem. Biophys 2004;422(2):161–7. [PubMed: 14759603]

[41]. Hersel U, Dahmen C, Kessler H. RGD modified polymers: biomaterials for stimulated cell adhesion and beyond. Biomaterials. 2003;24(24):4385–415. [PubMed: 12922151]

[42]. Cui YL, Qi AD, Liu WG, Wang XH, Wang H, Ma DM, et al. Biomimetic surface modification of poly(l-lactic acid) with chitosan and its effects on articular chondrocytes in vitro. Biomaterials. 2003;24(21):3859–68. [PubMed: 12818559]

[43]. Baker MI, Walsh SP, Schwartz Z, Boyan BD. A review of polyvinyl alcohol and its uses in cartilage and orthopedic applications. Journal of biomedical materials research. Part B, Applied biomaterials. 2012;100(5):1451–7.

[44]. Black JP, Sefton MV. Complement activation by PVA as measured by ELIFA (enzyme-linked immunoflow assay) for SC5b-9. Biomaterials. 2000;21(22):2287–94. [PubMed: 11026635]

[45]. Burczak K, Gamian E, Kochman A. Long-term in vivo performance and biocompatibility of poly(vinyl alcohol) hydrogel macrocapsules for hybrid-type artificial pancreas. Biomaterials. 1996;17(24):2351–6. [PubMed: 8982475]

[46]. Cartiva.net [internet]. Memphis, TN: Wright Medical Group N.V.; [cited 2018 12 20] Available from: https://cartiva.net/

[47]. Maher SA, Doty SB, Torzilli PA, Thornton S, Lowman AM, Thomas JD, et al. Nondegradable hydrogels for the treatment of focal cartilage defects. Journal of biomedical materials research. Part A. 2007;83(1):145–55.

[48]. Krych AJ, Wanivenhaus F, Ng KW, Doty S, Warren RF, Maher SA. Matrix generation within a macroporous non-degradable implant for osteochondral defects is not enhanced with partial enzymatic digestion of the surrounding tissue: evaluation in an in vivo rabbit model. J. Mater. Sci. Mater. Med 2013;24(10):2429–37. [PubMed: 23846837]

[49]. Jones CM, Donnelly PE, Schwartz J. A nanoscale interface improves attachment of cast polymers to glass. ACS applied materials & interfaces. 2010;2(8):2185–8. [PubMed: 20690771]

[50]. Lamour G, Hamraoui A, Buvailo A, Xing Y, Keuleyan S, Prakash V, et al. Contact Angle Measurements Using a Simplified Experimental Setup. J. Chem. Educ 2010;87(12):1403–7.

[51]. Schneider CA, Rasband WS, Eliceiri KW. NIH Image to ImageJ: 25 years of image analysis. Nat. Methods 2012;9(7):671–5. [PubMed: 22930834]

[52]. Brugnara M, Volpe CD, Siboni S, Zeni D. Contact angle analysis on polymethylmethacrylate and commercial wax by using an environmental scanning electron microscope. Scanning. 2006;28(5): 267–73. [PubMed: 17063765]

[53]. Chen T, Buckley M, Cohen I, Bonassar L, Awad HA. Insights into interstitial flow, shear stress, and mass transport effects on ECM heterogeneity in bioreactor-cultivated engineered cartilage hydrogels. Biomechanics and modeling in mechanobiology. 2012;11(5):689–702. [PubMed: 21853351]

[54]. Harris GM, Madigan NN, Lancaster KZ, Enquist LW, Windebank AJ, Schwartz J, et al. Nerve Guidance by a Decellularized Fibroblast Extracellular Matrix. Matrix Biol. 2017;60:176–89. [PubMed: 27641621]

[55]. Bandini SB, Spechler JA, Donnelly PE, Lim K, Arnold CB, Schwarzbauer JE, et al. Perforation Does Not Compromise Patterned Two-Dimensional Substrates for Cell Attachment and Aligned Spreading. ACS Biomaterials Science & Engineering. 2017;3(12):3123–7.

[56]. Sennett ML, Meloni GR, Farran AJ, Guehring H, Mauck RL, Dodge GR. Sprifermin Treatment Enhances Cartilage Integration in an In Vitro Repair Model. Journal of Orthopaedic Research®. 2018.

[57]. van de Breevaart Bravenboer J, der Maur CDI, Bos PK, Feenstra L, Verhaar JA, Weinans H, et al. Improved cartilage integration and interfacial strength after enzymatic treatment in a cartilage transplantation model. Arthritis Res. Ther 2004;6(5):R469. [PubMed: 15380046]

[58]. Boushell MK, Hung CT, Hunziker EB, Strauss EJ, Lu HH. Current strategies for integrative cartilage repair. Connect. Tissue Res 2017;58(5):393–406. [PubMed: 27599801]

[59]. Watt FM. Effect of seeding density on stability of the differentiated phenotype of pig articular chondrocytes in culture. J. Cell Sci 1988;89(3):373–8. [PubMed: 3058725]

[60]. Gu ZQ, Xiao JM, Zhang XH. The development of artificial articular cartilage–PVA-hydrogel. Biomed. Mater. Eng 1998;8(2):75–81. [PubMed: 9830990]

[61]. Stammen JA, Williams S, Ku DN, Guldberg RE. Mechanical properties of a novel PVA hydrogel in shear and unconfined compression. Biomaterials. 2001;22(8):799–806. [PubMed: 11246948]

[62]. Caron MMJ, Emans PJ, Coolsen MME, Voss L, Surtel DAM, Cremers A, et al. Redifferentiation of dedifferentiated human articular chondrocytes: comparison of 2D and 3D cultures. Osteoarthritis Cartilage. 2012;20(10):1170–8. [PubMed: 22796508]

[63]. Baker BM, Chen CS. Deconstructing the third dimension–how 3D culture microenvironments alter cellular cues. J. Cell Sci 2012;125(13):3015–24. [PubMed: 22797912]

[64]. Kang JY, Chung CW, Sung J-H, Park B-S, Choi J-Y, Lee SJ, et al. Novel porous matrix of hyaluronic acid for the three-dimensional culture of chondrocytes. Int. J. Pharm 2009;369(1): 114–20. [PubMed: 19059468]

[65]. Sanz-Ramos P, Mora G, Vicente-Pascual M, Ochoa I, Alcaine C, Moreno R, et al. Response of Sheep Chondrocytes to Changes in Substrate Stiffness from 2 to 20 Pa: Effect of Cell Passaging. Connect. Tissue Res 2013;54(3):159–66. [PubMed: 23323769]

[66]. Chen C, Xie J, Deng L, Yang L. Substrate Stiffness Together with Soluble Factors Affects Chondrocyte Mechanoresponses. ACS applied materials & interfaces. 2014;6(18):16106–16. [PubMed: 25162787]

[67]. Yamaura K, Tada M, Tanigami T, Matsuzawa S. Mechanical properties of films of poly (vinyl alcohol) derived from vinyl trifluoroacetate. J. Appl. Polym. Sci 1986;31(2):493–500.

[68]. Kim J, Cho D-iD, Muller RS. Why is (111) silicon a better mechanical material for MEMS? Transducers' 01 Eurosensors XV: Springer; 2001 p. 662–5.

[69]. Morgan JR, Yarmush ML. Tissue engineering methods and protocols: Springer Science & Business Media; 1998.

[70]. Wilson CJ, Clegg RE, Leavesley DI, Pearcy MJ. Mediation of Biomaterial–Cell Interactions by Adsorbed Proteins: A Review. Tissue Eng. 2005;11(1–2):1–18. [PubMed: 15738657]

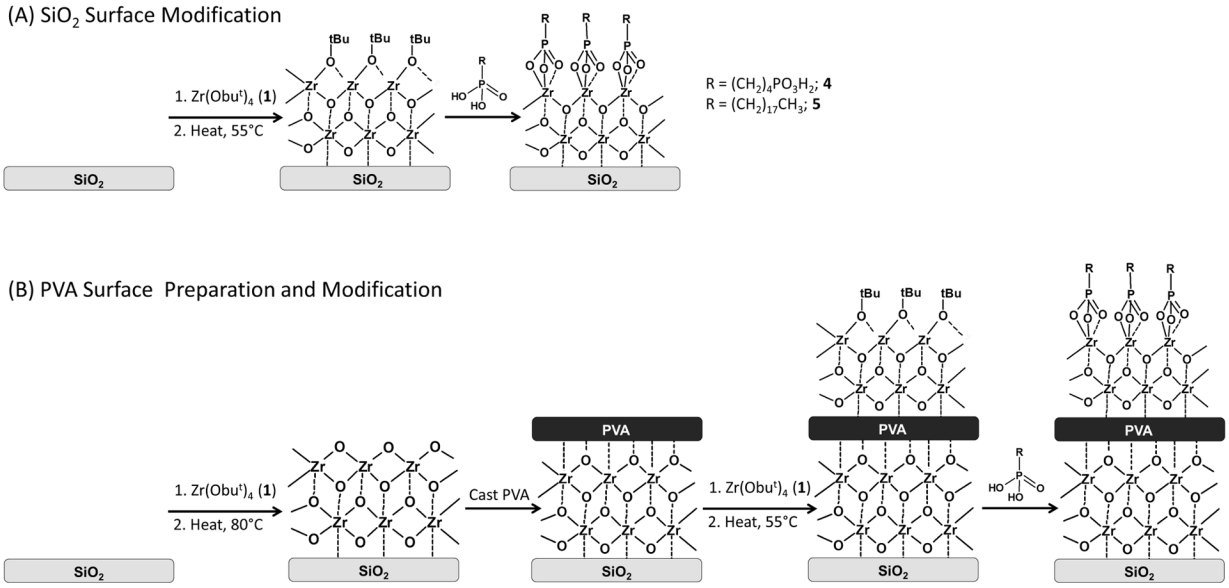

Figure 1.

SAMP surface modification scheme. (A) SiO_2 surface modification: clean SiO_2 is exposed to **1** vapor and then gently heated to 55° C to form a mixed Zr oxide/alkoxide layer (**2**). The **2**-terminated SiO_2 is then immersed in an ethanol solution of a phosphonic acid to yield SAMP-terminated SiO_2. (B) PVA film fabrication and surface medication: clean SiO_2 is exposed to **1** vapor and then heated to 80° C to form a ZrO_2 layer (**3**). The **3**-terminated SiO_2 is spin-cast with PVA from a formic acid solution to yield a PVA thin film supported on a **3**-terminated SiO_2 substrate. The PVA film is exposed to **1** vapor and gently heated to 55° C to form a mixed Zr oxide/alkoxide layer, and is then immersed in an ethanol solution of a phosphonic acid to yield a SAMP-terminated PVA film surface. Note: this schematic is not meant to imply any particular stoichiometry.

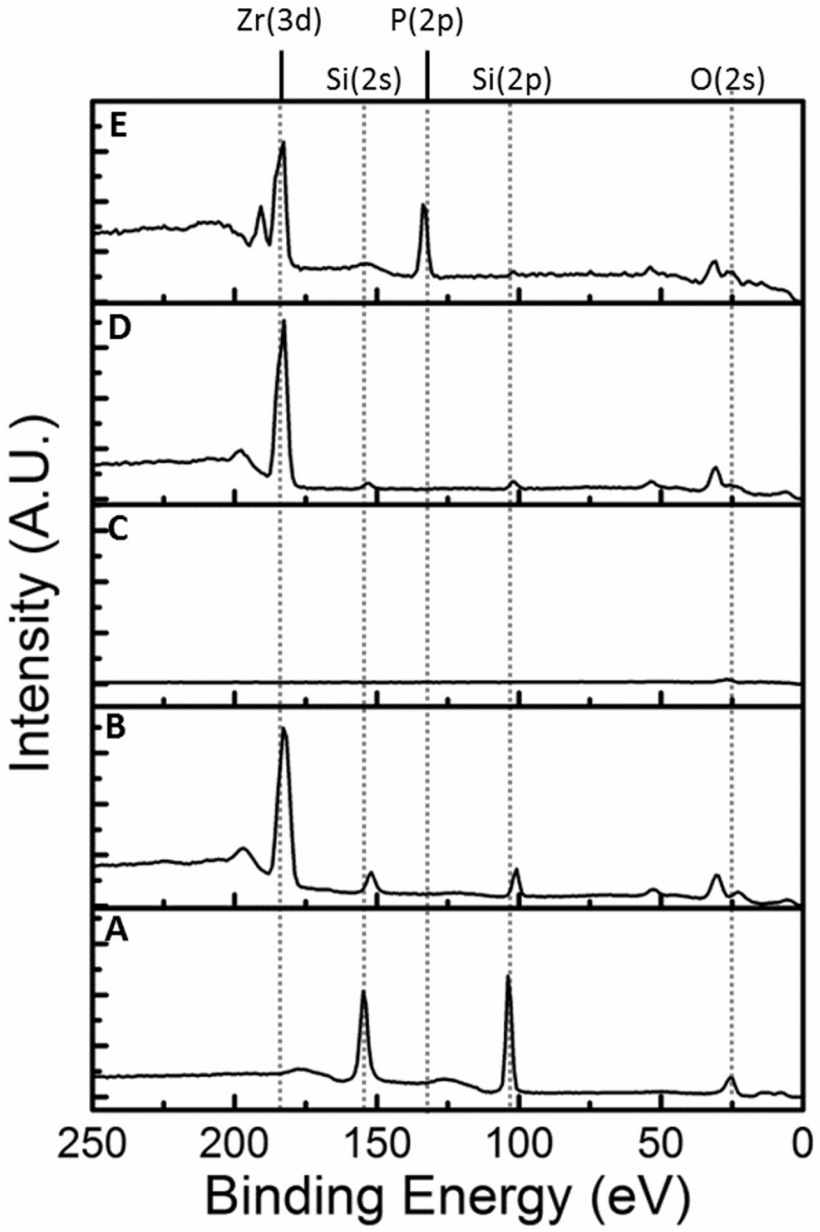

Figure 2.

XP spectra for the process of **4**-terminated PVA synthesis starting from clean SiO_2, refer to Figure 1B for PVA film fabrication and surface modification. (A) clean, unmodified SiO_2, (B) **3**-terminated SiO_2, (C) PVA thin film (~ 123 nm) on **3**-terminated SiO_2, (D) **3**-terminated PVA thin film, (E) **4**-terminated PVA thin film. Note the appearance of the Zr(3d) after chemical vapor deposition steps and the appearance of the P(2p) after SAMP modification.

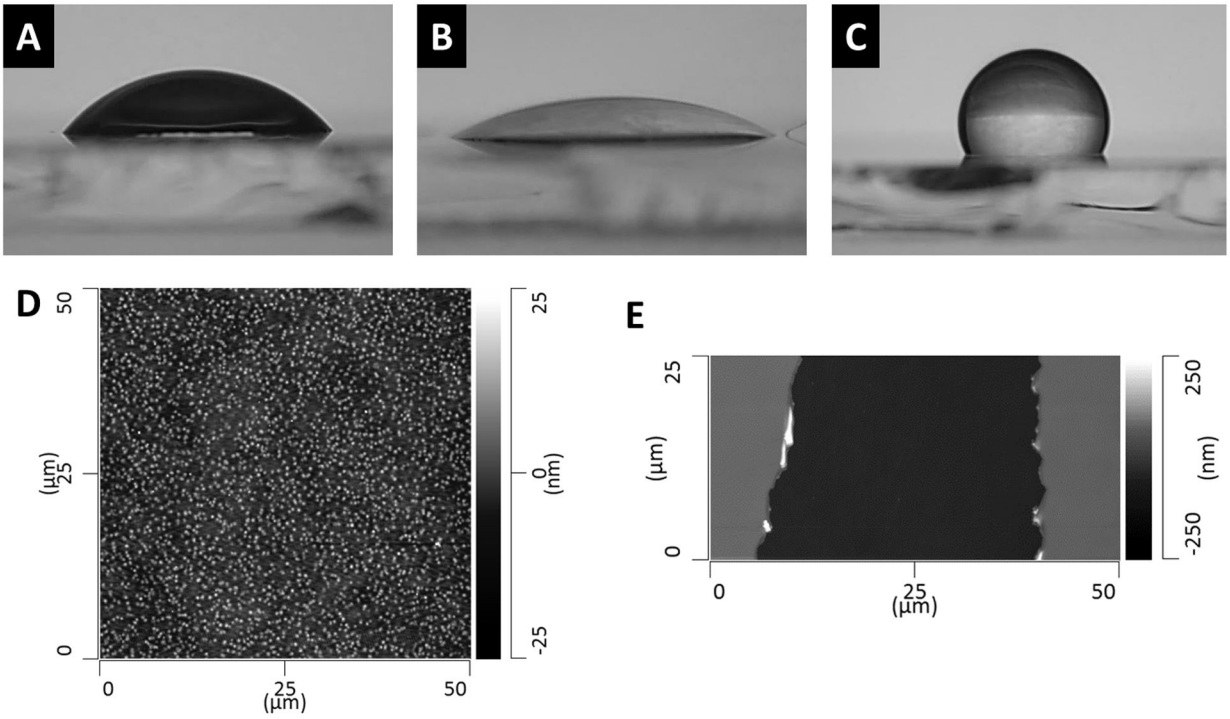

Figure 3.

Contact angle goniometry and atomic force microscopy performed on PVA thin films. Contact angle of water on (A) unmodified PVA thin film, 56°; (B) **4**-terminated PVA, < 20°; (C) **5**-terminated PVA, > 100°; (D) AFM height image of unmodified PVA thin film (50 μm x 50 μm ROI), average roughness of PVA thin films = 3.5 nm ± 0.7 nm; (E) AFM height image of a PVA thin film with a scratch to determine film thickness, average PVA thin film thickness = 123 nm ± 2 nm. Averages are reported as average ± 1 standard deviation from 5 measurements from 5 different images.

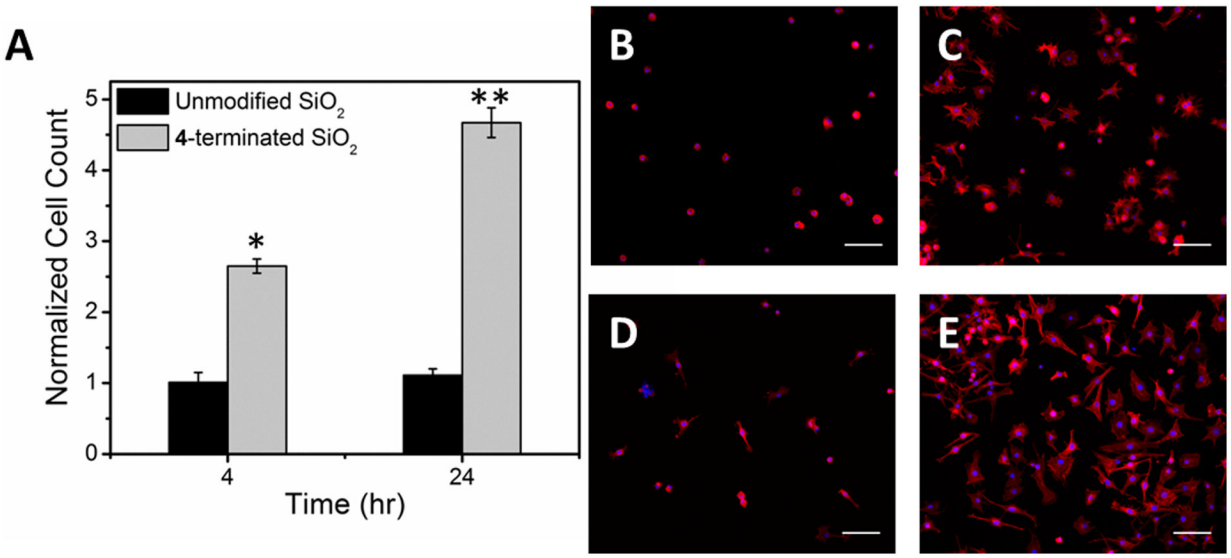

Figure 4.

Primary mature bovine chondrocytes on **4**-terminated and unmodified SiO_2 surfaces. (A) Normalized cell count, all data are normalized to the 4 hr count on unmodified SiO_2. Data are reported as average ± 1 S.E. ($n \geq 16$). Images, 20x, of chondrocytes stained with rhodamine phalloidin (red) and DAPI (blue) on (B) unmodified SiO_2 after 4 hr, (C) **4**-terminated SiO_2 after 4 hr, (D) unmodified SiO_2 after 24 hr, and (E) **4**-modified SiO_2 after 24 hr.(*) denotes statistical difference from the 4 hr control and (**) denotes statistical difference from the 24 hr control; scale bars = 100 μm.

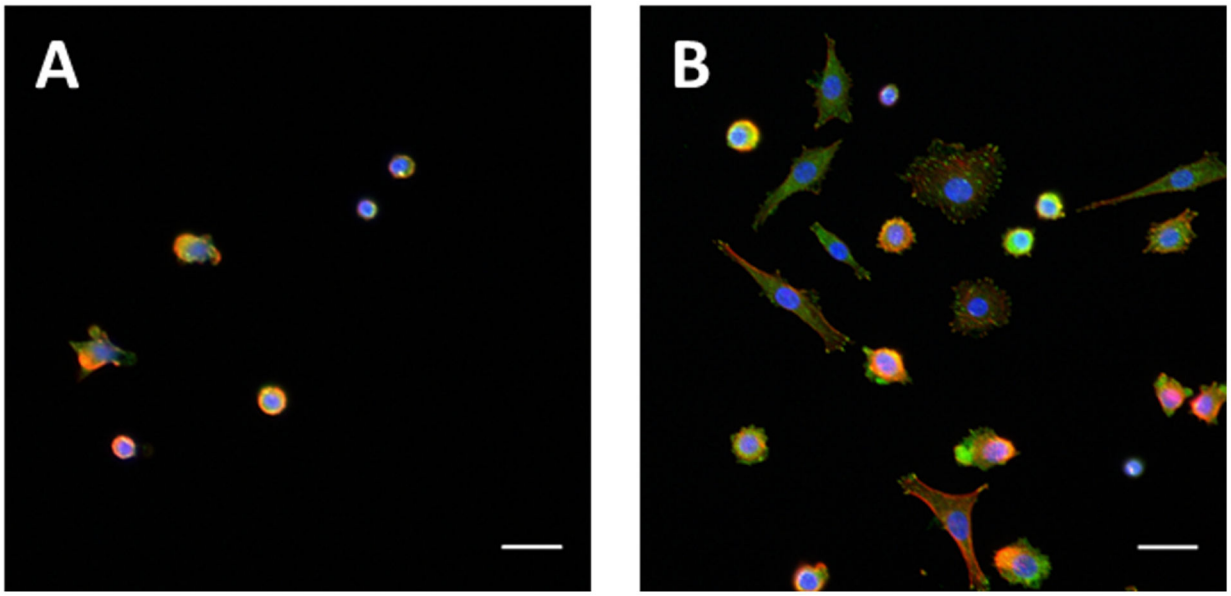

Figure 5.

Primary mature bovine chondrocytes on **4**-terminated and unmodified SiO_2 surfaces after 24 hr. Images are magnified 20x micrographs of cells stained with rhodamine phalloidin (red), DAPI (blue), and an anti-vinculin antibody (green) on (A) unmodified SiO_2 and (B) **4**-terminated SiO_2; scale bars = 25 μm. Note the focal adhesion formed on the chondrocytes that have begun to spread.

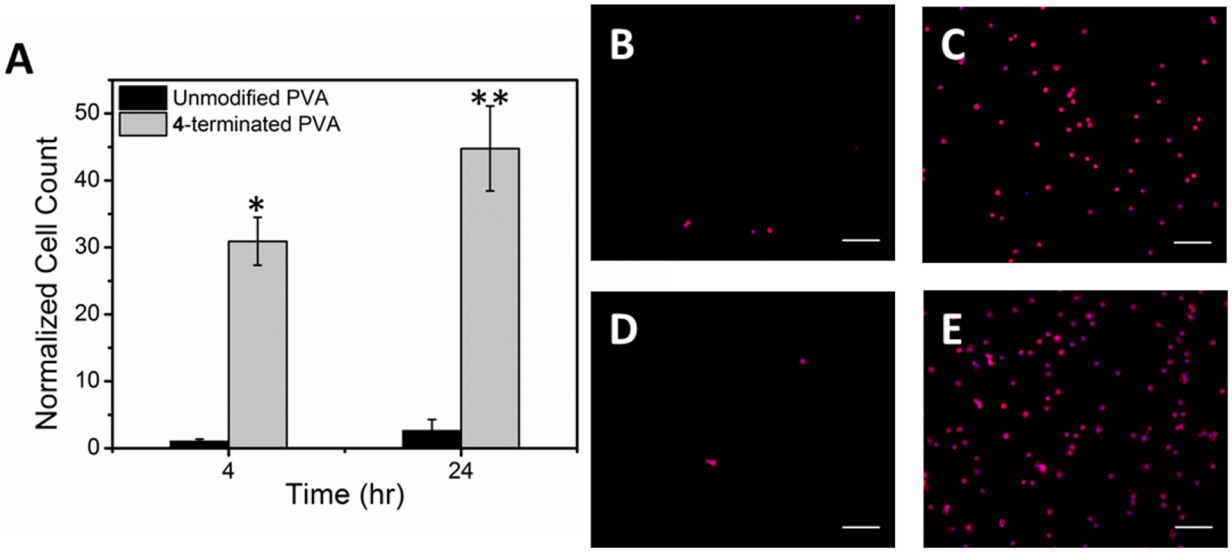

Figure 6.

Primary mature bovine chondrocytes on **4**-terminated and unmodified PVA thin film surfaces. (A) Normalized cell count, all data are normalized to the 4 hr count on unmodified PVA. Data are reported as average ± 1 S.E. ($n \geq 16$). Images, 20x, of chondrocytes stained with rhodamine phalloidin (red) and DAPI (blue) on (B) unmodified PVA after 4 hr, (C) **4**-terminated PVA after 4 hr, (D) unmodified PVA after 24 hr, and (E) **4**-modified PVA after 24 hr.(*) denotes statistical difference from the 4 hr control and (**) denotes statistical difference from the 24 hr control; scale bars = 100 μm.

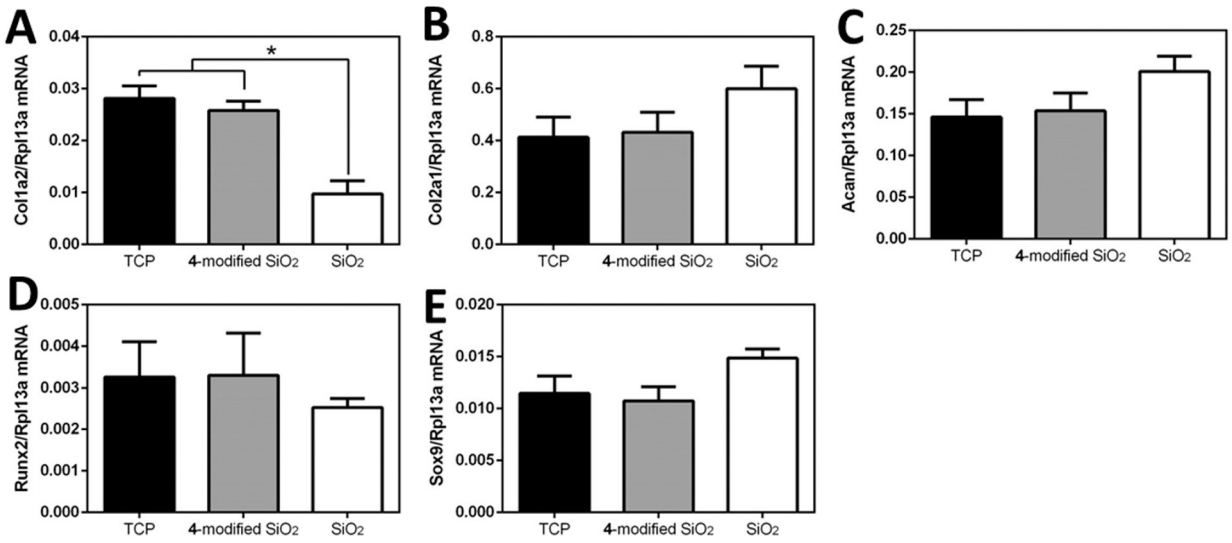

Figure 7.

Gene expression of primary mature bovine chondrocytes on **4**-terminated and unmodified SiO_2 surfaces. RNA was collected from cells after 3 days of culture on either tissue culture plastic (C), **4**-terminated (C4), or unmodified SiO_2 surfaces (SiO2) for the following genes A) Col2a1, B) Col1a2, C) Acan, D) Sox9, and E) Runx2. All genes of interest were normalized to Rpl13a. * denote significant differences ($p<0.05$).

Table 1.

Bovine primers for genes of interest.

Gene	Forward Primer (5'–3')	Reverse Primer (5'–3')
Rpl13a	GCCTACTCGCAAGTTTGCCT	GCCGTTACTGCCTGGTACTT
Acan	GGGAGGAGACGACTGCAATC	CCCATTCCGTCTTGTTTTCTG
Col1a2	ACATGCCGAGACTTGAGACTCA	GCATCCATAGTACATCCTTGGTTAGG
Col2a1	GCTTCCACTTCAGCTATGGA	CAGGTAGGCAATGCTGTTCT
Runx2	AGTGATTTAGGGCGCATTCCT	GAGGGCCGTGGGTTCTG
Sox9	ACGCCGAGCTCAGCAAGA	CACGAACGGCCGCTTCT